The Cryosphere Discuss., 7, 6043–6074, 2013
www.the-cryosphere-discuss.net/7/6043/2013/
doi:10.5194/tcd-7-6043-2013

The Cryosphere
Discussions
Open Access

Surface kinematics of periglacial sorted circles using Structure-from-Motion technology

A. Kääb[1], L. Girod[1], and I. Berthling[2]

[1]Department of Geosciences, University of Oslo, P.O. Box 1047, Oslo, Norway
[2]Department of Geography, Norwegian University of Science and Technology,
7491 Trondheim, Norway

Received: 26 November 2013 – Accepted: 29 November 2013
– Published: 18 December 2013

Correspondence to: A. Kääb (kaeaeb@geo.uio.no)

Published by Copernicus Publications on behalf of the European Geosciences Union.

Abstract

Sorted soil circles are a conspicuous form of periglacial patterned ground. Numerical modelling suggests that these features develop from a convection-like circulation of material in the active layer of permafrost. The related iterative burying and resurfacing of material is believed to play an important role in the soil carbon cycle of high latitudes. The connection of sorted circles to permafrost conditions and its changes over time make these ground forms to a potential paleoclimatic indicator. In this study we apply the photogrammetric Structure-from-Motion technology (SfM) to large sets of overlapping terrestrial photos taken in Augusts 2007 and 2010 over three sorted circles at Kvadehuksletta, Western Spitsbergen. We retrieve repeat digital elevation models (DEMs) and orthoimages with millimetre-resolution and accuracy. Changes in microrelief over the three years are obtained from DEM-differencing and horizontal displacement fields from tracking features between the orthoimages. In the inner domains of the circles, consisting of fines, material moves radially outside with horizontal surface speeds of up to 2 cm yr^{-1}. The outer circle ridges consist of coarse stones that displace towards the inner circle domain at similar rates. A number of substantial deviations from this overall radial symmetry, both in horizontal displacements and in microrelief, shed new light on the potential spatio-temporal evolution of sorted soil circles, and periglacial patterned ground in general.

1 Introduction

The term patterned ground describes a range of small-scale landforms such as polygons, stripes and circles, found in periglacial environments (Washburn, 1980). Patterned ground develops in frost-susceptible soils due to repeated actions of seasonal freezing and thawing. These landforms are considered an excellent geomorphic example of self-organization and emergence in complex systems (e.g. Kessler et al., 2001; Kessler and Werner, 2003). The most prominent forms of this type are found in the active layer of Arctic or Antarctic lowland permafrost, where the permanently frozen subsurface confines water and creates special hydrological conditions in the overlying layer of seasonal freezing and thawing, the so-called active layer.

The most conspicuous type of patterned ground is sorted circles. They consist of a core of fine-grained material, reaching a depth of at least the active layer, which is surrounded by a much coarser circular border or ridge of open-work fabric that extends some decimetre above the centre surface (Fig. 1). Typical diameters for the fine-grained centre are 1–3 m while the coarse elevated border may be 0.5–1 m wide. Much smaller forms are also found (e.g. Matsuoka et al., 2003). The surface material in the centre domain shows a radial outward movement on the order of 0.01 $\mathrm{m\,yr^{-1}}$ (Schmertmann and Taylor, 1965; Hallet and Prestrud, 1986), and from measuring the tilt of inserted rods it is assumed that a similar inward movement takes place at depth (Hallet, 1998). For mass continuity reasons, this suggests that the fine material within the centre follows a displacement pattern similar to a convection cell. This burial – and later resurfacing – of material in patterned ground is an important element within the soil carbon cycle of high latitudes (e.g. Bockheim, 2007; Horwath et al., 2008) as well as soil development (e.g. Bockheim et al., 1998) and highlights that precise knowledge about patterned ground dynamics has implications far beyond the geomorphic interest in process/form relationships – especially with respect to the effect of warmer air and ground temperatures on soil carbon stocks. Moreover, patterned ground is considered a potential paleoclimatic indicator based on the expected relation between pattern size and permafrost conditions such as active layer depth (Hallet and Prestrud, 1986).

A variety of mechanisms have been suggested for the origin of sorted circles and other patterned-ground landforms (cf. Washburn, 1980), but recent work focusses on differential frost heave (e.g. Peterson, 2008), and its feedback with progressive sorting (e.g. Kessler et al., 2001; Kessler and Werner, 2003). Scientific progress within this field is due to a combination of thorough field investigations, laboratory work and theoretical studies (Hallet, 1998), and has led to numerical models describing the development of unsorted circles (Peterson and Krantz, 2008), and sorted circles and other sorted patterned-ground landforms (Kessler et al., 2001; Kessler and Werner, 2003). In the model of Kessler and Werner (2003), two main mechanisms determine the development of circles from the starting point of a stone layer above fine-grained soil. First, fine material and stones are transported in opposite directions normal to the freezing front during freeze-thaw cycles, with a lateral component due to the differential freeze-thaw. Second, as stones through time are thus sorted into elongated regions, the stone domains are progressively squeezed by the fine domains during winter freeze-up, when the rapidly cooling stone domain causes lateral frost heave within the fine domain. The effect of the second mechanism is stone transport along the long axis of the stone domains. Pattern types change in model runs due to increasing slope (causing stripes to develop), decreasing stone concentration (leading to stone labyrinths and stone islands), and increasing lateral confinement (favouring polygonal patterns).

The model of Kessler and Werner (2003) can be considered an hypothesis for the main mechanisms involved in patterned-ground formation. It provides specific predictions about the dynamics of centre and border domains. However, empirical data of sorted circle dynamics consist so far only of point measurements (e.g. Hallet and Prestrud, 1986; Hallet, 1998), while measurements of the three-dimensional surface displacement fields should be feasible today – even over short timescales. Such data would be better suited to test these predictions. Questions arise also if and how the dynamics of the circles might be influenced by changes in the underlying frozen ground, such as changes in its thermal properties and structure, and related impacts on the ground hydrology. A comprehensive benchmark of present-day dynamics would aid research on this subject, which is linked to the potential importance of cryoturbation and differential frost heave in the global carbon cycle. Ultimately, better understanding of the processes involved in the dynamics of patterned ground and their changes over time would facilitate their use as indicator for present and past environmental conditions in cold regions. Our objective is thus to test a methodology for deriving the 3-D surface kinematics of sorted circles, and to analyse such initial data with respect to predictions from conceptual and numerical models.

Title Page
Abstract | Introduction
Conclusions | References
Tables | Figures
◀| |▶
◀ ▶
Back | Close
Full Screen / Esc
Printer-friendly Version
Interactive Discussion

To quantify the surface kinematics of selected sorted circles we apply the Structure-from-Motion (SfM) technology to a multi-temporal set of terrestrial images to derive vertical and horizontal components of change over time. SfM combines well-established photogrammetric principles, in particular bundle adjustment and image matching, with modern computational methods to arrive at a powerful and user-friendly software environment that is able to extract a three-dimensional model from a set of images, which then forms the base for a range of further products, among them digital elevation models (DEMs) and orthoimages. The SfM technology proofed already very powerful for a large range of geoscientific applications, such as geological and glaciological studies, coastal erosion, river morphology, volcanic activity, or landsliding (e.g. Girod, 2012; James and Robson, 2012; Westoby et al., 2012; Fonstad et al., 2013).

2 Method

2.1 Study site and data collection

For our study we selected a series of three adjacent sorted circles at Kvadehuksletta, Brøggerhalvøya, Western Spitsbergen (Fig. 1). The overall elevation level asl. of the circles studied is around 53 m a.s.l. The sorted circles at Kvadehuksletta are among the best-developed of their kind on Earth, as far as known to us, and comparably easy to access 10 km to the southeast from the Ny-Ålesund research station, and with the Geopol hut in close vicinity. As a result, these circles have been subject to a number of earlier investigations (Hallet and Prestrud, 1986; Anderson, 1988; Hallet et al., 1988; Etzelmuller and Sollid, 1991; Hallet, 1998; Putkonen, 1998) (see also Sect. 1), and a detailed geomorphological map is also available (Tolgensbakk and Sollid, 1987).

Kvadehuksletta is a wide strandflat, covered with beach deposits of Holocene and older age. Our study site is situated above the lateglacial marine limit. Bedrock in the area consists of dolomite, and most of the beach-ridge stones are of local origin. Due to weathering of the dolomite and subsequent eluviation, a frost-susceptible silty fine material has developed at shallow depth (Etzelmuller and Sollid, 1991), which facilitates exactly the starting point of the Kessler and Werner (2003) model for development of sorted circles. Large areas between the beach ridges are covered by such sorted circles, grading in some areas towards sorted polygons and, more irregular sorted forms as well as stripes on slopes (Tolgensbakk and Sollid, 1987). The fine inner domains of the circles often have a variable cover of vegetation, mainly dominated by cryptogamic crust, that gives the inner circle a dark appearance, but sometimes also with higher vegetation such as sedges and salix. The vegetation tends to be densest close to stone borders, and shows evidence of the surface movement pattern. Even in the stone domains, salix is found. Climatic data are available from Ny-Ålesund, where mean annual air temperature is −6.3 °C and mean annual precipitation is 385 mm for the normal period 1961–1990. Recent warming in the Arctic areas suggests that these values may not necessary be fully representative any longer for the present situation (Isaksen et al., 2007a, b), and in Fig. 2 the mean monthly anomaly from the normal, calculated for the period 1991–2010, provides a more realistic picture of the present climatic situation at the site. The anomaly is most pronounced in winter. Figure 2 also displays air temperatures during the study period and melting season degree day sums, and near surface temperatures 1999–2010 (7 day running mean) from the 15 m deep Jansonhaugen borehole near Longyearbyen (K. Isaksen, personal communication, 2013). The recent warming causes warmer ground temperatures and deeper active layer at the Janssonhaugen site, and this is presumeably also the case at Kvadehuksletta. Apart from the unusual warm winter of 2005–2006 (Isaksen et al., 2007a), no extreme events likely to influence our measurements are recorded in these data.

Field visits were undertaken in Augusts 2007 and 2010. We used a ca. 3 m high ladder in different positions to collect a large number of overlapping images over the adjacent three circles studied. For both acquisition campaigns, a Canon EOS 10D camera with 3072 × 2048 pixels was used with a fixed focal length of 20 mm. On 9 August 2007 63 images were taken, and 104 on 14 August 2010.

As ground control points, ten ca. 10 cm long metal bolts with a round metal plate mounted on top of them were pushed in the ground until the top plate reached the ground level. The points were well distributed over the site imaged (Fig. 2). At both campaigns, in 2007 and again in 2010, the position of these control points was surveyed using differential the Global Navigation Satellite System (GNSS) relative to a mark in a rock close to the Geopolen hut (Fig. 1). In 2010, the bolt plates were heaved by a few centimetres and had to be pressed down back to ground level in order to be stable enough for setting the GNSS antenna on them. The absolute position of the ground control network in UTM coordinates, here less of a concern than the relative accuracy between both acquisition campaigns, was determined by linking the local GNSS measurements through a code-based correction to the fundamental geodetic station in Ny-Ålesund. The GNSS network adjustments suggest a relative accuracy of the control points of a few millimetres. Though, the facts that (i) the bolts had to be fixed again before the 2010 measurement, that (ii) GNSS elevation is often less well determined than horizontal GNSS position (in particular in high latitudes with low satellite altitude angles), and that (iii) the reference rock at Geopolen hut is not bedrock and its position thus also expected to be affected by frost processes, prevents drawing sound conclusions from the GNSS positions between 2007 and 2010, and thus for absolute horizontal and vertical displacements of the studied circles as a whole. Rather, vertical and horizontal changes were analysed as relative displacements between the 2007 and 2010 images.

2.2 Image processing

For both campaigns separately, the ladder images were combined to a three-dimensional model using the Structure-from-Motion (SfM) technology (see Sect. 1 and e.g. James and Robson, 2012; Westoby et al., 2012; Fonstad et al., 2013). SfM does not require the position and looking direction of the camera, or alternatively the 3-D position of control points, to be known before constructing a point cloud based on a series of overlapping images. Independent 3-D positions of control points recognizable in the point cloud are in a later step necessary to enable the absolute orientation. Here, we used the software MicMac (Pierrot-Deseilligny and Clery, 2011, 2012; MicMac, 2013a, b), and processing consisted of the following, mostly fully automatic steps:

1. find a set of corresponding points (tie points) between images using the SIFT algorithm (scale-invariant feature transform);
2. compute the position and orientation of the viewpoints, as well as the camera's internal parameters (focal length, distortion, etc.) through bundle adjustment;
3. record the position of the GCPs (ground control points) in the images (2-D coordinates in pixels) and transform the GCP absolute coordinates in an Euclidian projection system (a local tangential coordinate system is commonly used);
4. scaling and rotation of the viewpoint positions and orientations are performed using the information of steps 2 and 3;
5. based on the data from step 4, a dense correlation is performed. It computes the 3-D positions of each point that can be seen in two or more images through the intersection of projection rays. The result of this step is a georeferenced depth map;
6. the images are then projected on the depth map, producing an orthoimage and a point cloud of the scene.

This process was performed for the image sets of 9 August 2007 and 14 August 2010. From the resulting point clouds of approximately 30 million points each, DEMs and orthoimages of 1 mm horizontal resolution were produced (Figs. 3 and 4). For most analyses, however, the DEMs and orthoimages were resampled to 2 mm resolution to speed up computations and display. For visualization and some analyses also 1 cm, 2 cm and 5 cm versions were produced.

Vertical differences between the 2007 and 2010 DEMs were obtained by simple subtraction. The two point clouds turned out to be vertically deformed to each other by a few centimetres at the eastern and southern margins (approximately from the top of the outer ridge of the circles eastwards and southwards towards the model margins). This deformation could not be repaired in the photogrammetric processing, mainly due to insufficient image coverage and constellations at the western and southern model margins. Rather, this effect was in parts compensated by applying a very coarse low-pass filter to the elevation differences and removing the filter results from the raw differences. Though, elevation differences towards to eastern and southern model margins have to be interpreted with care.

Horizontal displacements between the two orthoimages were determined through offset tracking. Using the free software CIAS (Correlation Image Analysis Software; Kääb and Vollmer, 2000; Heid and Kääb, 2012; Kääb, 2013) and its normalized cross-correlation and orientation correlation algorithms, a 5 cm-spaced grid of displacements was measured based on 10 cm-sized image templates. This large template size, compared to the high image resolution, turned out to be necessary to cope with the often individually moving, rotating, or tipping stones that led in parts to a low visual coherence between the two images. The DEM deformations mentioned above also had an effect on the orthoimages at the southern margin of the photogrammetric model, but only a small effect towards the eastern model margin. As a result, the displacements on the southernmost circle were measured separately from the other two circles after independent co-registration of the two orthimages using points at the ridge top where displacements are assumed minimal. As for the DEM differences, though, the displacements towards the eastern and southern model margins have to be interpreted with care as they could be affected by model distortions of low spatial frequency.

The DEMs retrieved are so dense (1 mm resolution) that interpolating the elevation both for the starting and endpoints of displacement vectors is expected to largely reflect the actual vertical component of particle motion.

3 Results

Elevation differences of control points between 2007 and 2010 cannot be analysed for reasons described above. The average horizontal offset between the 2007 and 2010 control points is about 1 cm, with only one offset > 1.5 cm (3 cm). We believe that holding the GNSS receiver on the control point marks causes a horizontal uncertainty of at least 1 cm. The offset directions give no systematic picture. For this reason, we conclude that the GNSS offsets between 2007 and 2010 are random, and cannot be interpreted geophysically.

3.1 Elevation models and differences

The 2007 and 2010 DEMs offer a large level of detail where, for instance, individual stones can easily be recognized (Figs. 3 and 4). Using some control points that have not been used for absolute orientation as check points, we obtain a standard deviation for elevation of ±6 mm (±2 mm yr^{-1}), which we consider to be a reasonable estimate for the vertical accuracy of the DEMs.

The deepest points of the circles are the outermost zones of the inner domain (Figs. 3 and 5). The circle centres are up to approximately 10 cm higher than these lowermost parts. The outer ridges have maximum heights of about 20–25 cm above the lowermost parts of the inner domains. The northern circle lies roughly 8 cm lower than the middle circle and 13 cm lower than the southern circle, measured as differences between the maximum elevations of inner fine domains (∼ centre of inner part).

The 1–2 mm resolution of the DEMs enables recognition of features that are otherwise difficult to detect and map, for instance cracks that are found both on the inner domains and ridges (Fig. 3).

Relative to the overall elevation level of about 53 m a.s.l. as defined by the control points, the highest zones in the circle centres are stable in elevation or rose by up to 0.7 cm yr^{-1} during the measurement period (Fig. 5). Most zones of the inner fine domain, in particular its outer margins, as well as the lower parts of the inside flanks of the coarse-grained ridges lower consistently, by up to 1.5 cm yr^{-1}. The ridges are stable in elevation or rise by up to 1.5 cm yr^{-1}. For most cracks, both on the ridges and in the inner parts of the circles, slight elevation losses indicate opening and lowering of the crack centre.

3.2 Orthoimages and displacements

The 2007 and 2010 orthimages allow for a variety of qualitative and quantitative analyses. The diameter of the inner, fine-grained domain of the northern circle is about 1.8 m, about 1.6 m for the middle one, and about 1.5 m for the southern circle. Typical stone b-axes on the outer rings range from 1–3 cm, with both smaller and larger ones, though. The larger stones tend to be found at the foot of the inner slope of the outer rings, whereas the smaller ones dominate the ridge tops, which partially also are composed of finer, sandy material (Fig. 4). The material on the outer rings appears freshly exposed with no signs of stable surface conditions such as lichens or weathering. The surface of the inner domains consists mainly of fines, with scattered stones of typical diameters around 1 cm. Accurate mapping of the delineation between inner circle fine domains and coarse stones of the outer rings does not reveal any systematic changes between 2007 and 2010. Local changes of this margin over the 3 yr observational period are mainly governed by displacing or tipping stones.

The strikingly high success rate of image correlations over the inner circle parts points to a very coherent deformation over the 3 yr observational period. This is confirmed by flickering the 2007 and 2010 orthoimages that also suggests a high visual coherence between both data sets. Maximum horizontal surface displacement rates reach 2 cm yr^{-1} for the inner part of the northern circle, 1 cm yr^{-1} for the middle circle, while only 3–4 mm yr^{-1} for the southern circle (Fig. 6). Overall, for the inner parts of all three circles the point displacement is radial and outwards. For the northern and middle circles, velocity magnitudes increase away from the centre. The displacement field of the middle circle has one clear centre with zero displacements. Such a centre is less clear for the northern circle, which has, in contrast to the middle circle, two zones with highest elevations, separated by a crack. The displacements on the southern circle are too small to accurately identify the centre of the radial displacements. The centres of the radial displacement fields seem to not exactly coincide with the highest points of the inner parts of the circles, with horizontal offsets of around 20–30 cm between both. The inner part of the northern circle shows a less homogenous radial displacement field than the middle circle, with scattered zones of comparable high speeds.

The ratio between speed (scaled to the range $[0,1]$) and the sinus of surface slope is for large zones of the inner parts of the circles several times larger than for the ridge flanks, typically 2–3 times as large, up to 20 times for the western part of the northern circle. In other words, for a given slope the surface displacements are much larger in the inner parts of the circles than for the outer rings.

The displacement field on the ridges is much less coherent than on the inner parts of the circles. Maximum horizontal speeds on the outer rings reach 1.5–2.5 $\mathrm{cm\,yr^{-1}}$, roughly towards the direction of steepest descent. Speeds are smallest on the ridge tops (Fig. 6).

On average, the maximum correlation coefficients of image matching, i.e. the correlation values that define the most probable displacements, are clearly higher on the inner parts of the circle than on the ridges (Fig. 7). This indicates highly coherent deformation in the inner domains, vs. less coherent deformation on the ridges. In fact, orthoimage flickering confirms that displacements on the ridges are often due to individually sliding stones or groups of stones (Figs. 6 and 8). For that reason image matching using templates smaller than 10 cm × 10 cm as used here fails in particular on the ridge flanks. The signal-to-noise ratio (SNR) of image matches, that is the ratio between maximum correlation coefficient and the average correlation coefficients for each matching location within the search area, is roughly equal for the ridges and the inner circle parts. This reflects that the lower correlation on the ridges affects equally maximum and average correlation (Fig. 7). Though, the transition between inner circle parts and ridges exhibits strikingly low SNRs indicating that the correlations in this zone are much weaker defined than in other parts. Image flickering shows that the most dominant surface changes are in fact concentrated in these zones with stones falling from the ridge flanks and being deposited here, stones tipping over, and stones from the surface of the inner parts being incorporated into the ridge (Fig. 8).

Constructing streamlines through the velocity fields (Kääb et al., 1998) gives surface travel times (∼ surface ages), between the circle centres and the outer margin of the inner domains, i.e. the transition between inner domains and ridges, of up to on the order of 100 yr.

4 Discussion

4.1 Method

For extracting the 3-D surface displacement field of sorted circles, we used a highly automatic time-lapse ground-based photogrammetric approach that yielded point clouds with a spatial resolution of about 1–2 mm. The method proved to be very successful to measure vertical and horizontal changes over 3 yr, but suffers also from some problems. First, the differential GNSS measurements of ground control points were by an order of magnitude less accurate than the precision of the point cloud. The GNSS rover was mounted on a short rod that was held by hand at each control point, adding a random horizontal error of about 1 cm to the GNSS error margin due to slight movement of the rod within the measurement time interval that, however, is partly compensated for by GNSS network adjustment. The GNSS error in the vertical direction is more problematic with respect to our final results, and additional levelling of control points to fix their elevations with millimetre-precision might in the future solve the problems with vertical deformation between point clouds, such as to the southwest margin of our models. Ground control point positioning errors cause problems with absolute orientation of the final models, and especially inhibit interpretation of sorted circle dynamics in areas of small displacements. Second, the image constellation chosen in the field was not optimized for SfM and sharp contrasts in the 2007 images from solar shadows also caused some problems for the photogrammetric model computation, in particular the SIFT algorithm.

Compared to the alternative solution of using a terrestrial laser scanner (TLS), photogrammetry offers somewhat higher resolution and precision, requires less equipment brought into the field, is much cheaper – but is more demanding with respect to data processing (cf. Westoby et al., 2012). TLS would require several scan positions in order to image outside/inside of sorted circles margins. Direct comparison of field data acquisition and DEM quality have been done by Westoby et al. (2012) and James and Robson (2012) who find the SfM technology faster in the field and of similar quality. However, TLS could have provided similar results as SfM in our study.

4.2 Circle dynamics

While interpreting our results about the surface kinematics of three sorted circles, two crucial uncertainties regarding temporal scale have to be considered, and apply to all of the below discussions. First, we observe these kinematics over three years, which might be a comparable short time period to the evolution time-scale of the circles (e.g. > 100 yr from our streamline estimate).It is thus open to which extent the 3 yr development measured is representative for the processes forming and maintaining the circles at longer time scales. Second, our change detection builds upon two points in time, namely two dates in Augusts, where the active layer is not at its deepest – judged from the degree day sum at the time of photography compared to the total sum the respective years (Fig. 2). It is thus also open to which extent the conditions of Augusts 2007 and 2010 are representative for annual average conditions or even for average August conditions (cf. Hallet, 1998). Short-term dynamics directly related to seasonal fluctuations in topography (from frost heave and thaw settlement processes) as well as stochastic variations in weather conditions are not picked up by our measurements. Under these restrictions, the initial, and perhaps most important geophysical finding in our study is that the microrelief of the circles is not stable through time. We observe an increase in relief during the measurement period, with increasing or stable elevation in fine domain centres and parts of the coarse borders, while the larger parts of the fine domains and especially the confluence between the coarse and fine domains decrease in elevation at rates of up to 1.5 $\mathrm{cm\,yr^{-1}}$ (relative between 2007 and 2010). This observation is counter-intuitive with respect to the similar visual appearance of the sorted circles with highly differing ages across different areas on Kvadehuksletta (Hallet and Prestrud, 1986), and in disagreement with the basic assumption of stable microrelief on which previous works (Hallet and Prestrud, 1986; Hallet et al., 1988; Hallet, 1998) base their calculations of vertical soil velocities.

A steadily increasing microrelief is, of course, not sustainable in the long run. This 2007–2010 topographic imbalance could have, again under the restrictions mentioned at the beginning of this section, internal or external reasons. The observed imbalance could actually be a recent trend, or circle-internal or externally-forced processes could lead to a topographic adjustment outside of our observation period.

Without associated measurements of environmental parameters our data cannot determine whether the changes in microrelief could be caused by stochastic variations in year to year climatic conditions or are part of a long term trend. There are no special events in the weather data from Ny-Ålesund during this period or in permafrost temperature data from Janssonhaugen in Adventdalen close to Longyeardalen (Fig. 2), and the degree day sum at the time of photography was larger in 2007 than in 2010. On the other hand, active layer monitoring data from Svalbard suggest increasing active layer thickness during the recent decade (Christiansen et al., 2010; Marsz et al., 2013) and the extremely warm winter-spring of 2005–2006 (Isaksen et al., 2007a) could have altered ground conditions for years.

Also, the observed increase in slope within the inner domain could, for instance, be compensated through time by sporadic events such as erosion due to heavy rain fall or snow melt, increased outward transport from conditions of high soil water content (external forcing), or natural modifications in the magnitude and pattern of the internal convection process (internal forcing). Our findings, over a limited time interval, though, suggest thus that a longterm-stable microrelief of the circles requires either external processes, or spatio-temporal variations of the internal processes, or combinations thereof.

Our results show that the areas of decreasing elevation constitute larger volumes than those that rise. It is therefore likely that the microrelief development is not, at least entirely, caused by the dynamics of the circles. Instead the decreasing elevation might also be caused by a thickening active layer accompanied by thaw settlement following ice melting in the transient zone. The elevation decrease and thaw settlement is not expected to be uniform, though, because ice melting also provides increased availability of soil water, and thus a potential for more frost heave and soil displacement during the yearly freeze-thaw cycle. Also differential freezing and thawing due to variable surface conditions, water content, thermal conductivity and advective heat transport, would influence this pattern. The areas where the relative elevation rises are areas where soil movement is predicted to have an upward velocity vector (Kessler et al., 2001). Further, in this model surface movement of soil is proportional to the local gradient. Accordingly, increasing surface relief will increase surface movement and therefore amplify the convection cell-like soil circulation within the sorted circles. This is similar as predicted for the general process of cryoturbation which may tend to increase sequestration of soil organic carbon (Bockheim, 2007), and thus act as a negative feedback in a global warming scenario.

Further to the change in microrelief we find that the general surface velocity field revealed in our data corresponds partly well to the point-based data from previous studies (Hallet and Prestrud, 1986; Hallet et al., 1988; Hallet, 1998) and to the predictions of the model by Kessler and Werner (2003). However, there are two important deviations. First, Kessler and Werner (2003) model fine-domain surface displacements as proportional to surface slope. The displacement fields of the three fine domains we investigate are, however, not well related to slope. In some sections, velocity vectors even point slightly upslope. These deviations from predictions could possibly be explained by differences in surface elevations during early summer thaw and the end of summer topography. Hallet (1998) reports frost heave during autumn of up to 10 cm in the centre of fine domain, and differential frost heave could then easily invert part of the relief during winter and early summer. Second, the difference we find in dynamic behaviour between neighbouring circles (of similar visual appearance) is striking and unexpected. In the southern circle, fine domain displacement is mainly at the lower detectable limit. The middle circle best displays surface velocity vectors pointing radially outwards roughly from the centre, in accordance with model predictions, but this origin of displacements surprisingly does not coincide with the highest topography within the fine domain. Again, it is unclear if the Augusts 2007 and 2010 topographies are representative of the topography under which largest seasonal displacements happen.

We further find an overall trend towards north north-east of the velocity vectors, and thus surface mass transport in this circle. The northern circle, however, has velocity vectors pointing mainly towards south west. Convergence between the northern and middle circle is also detected for the coarse borders. For the northern circle, stones on the north-eastern border cascade down along the steepest slope towards an area of the fine domain where there is negligible horizontal movement but strong subsidence. Elsewhere along this coarse domain, there is an along-border velocity component pointing towards south, especially on the western side where fine domain and coarse domain vectors converge almost perpendicular. A similar displacement field is found on the western side of the middle circle, but here the velocity component is pointing towards the northern circle. Thus, the convergence is not caused by a simple radial extension. It is also unrelated to overall slope of the area. Probably, the convergence is due to larger-scale variability of differential frost heave, governed by variability of parameters such as soil water content and snow accumulation. To some extent, the velocity patterns discussed in this paragraph could be due to low-frequency distortions in the photogrammetric bundle model. However, we believe that these patterns hold at least qualitatively, as they are partially of different shape than expected for such distortions, e.g. with sharp gradients.

Title Page
Abstract | Introduction
Conclusions | References
Tables | Figures
◀| |▶
◀ ▶
Back | Close
Full Screen / Esc
Printer-friendly Version
Interactive Discussion

For some parts of the borders, stones move downslope at an angle to the maximum slope. The effect is through time to displace borders in an along border direction, which is in accordance with the model by Kessler and Werner (2003).

Whereas our measurements of surface kinematics do not enable retrieving vertical fluxes directly, they allow though for indirect conclusions. Assuming, at least roughly, mass conservation and surface-parallel movement only, the surface velocity field should exhibit radially decreasing speeds due to the divergence of the field. Instead, speeds are zero or below the detection level in the circle centres, and also decreasing close to the outer border of the inner domains. For most parts of the inner domains speeds show no sign of outwards decrease. Thus, our measurements indicate that vertical emergence (upwelling) of material to compensate for horizontal divergence is expected for much of the inner domains, except very close to the border towards the outer ridges where submergence (downwelling) could happen. This, in turn, suggests that much of the material submergence happens actually hidden under the ridges. This way, our measurements, indirectly, confirm also the general up- and downwelling pattern predicted by Kessler and Werner (2003).

5 Conclusions

We apply for the first time the Structure-from-Motion technology (SfM) to periglacial patterned ground based on repeat terrestrial photography. This way we measure horizontal and vertical components of 3 yr surface displacements over three sorted soil circles at Kvadehuksletta, Spitsbergen, with an accuracy of a few millimetres. Our results confirm the large potential of SfM for in-situ studies of cryospheric and geomorphological surface processes and, specifically, that it is possible to extract high resolution 3-D surface displacement patterns of patterned ground features, even over relatively short timescales. The error estimates for vertical precision of the models are in the order of ±6 mm which is well below the actual relative displacements revealed for large parts of the investigated area.

Our results for horizontal velocities with rates of up to 2–3 cm yr^{-1} for both the inner, fine-domain parts of the circles and the outer, course-domain ridges around them on overall confirm model predictions (Kessler and Werner, 2003) of a radial convection cell-like circulation of inner parts, which drives also mass accumulation and turnover in opposite rotation direction on the outer rings (Fig. 9). Also in agreement with this model, high values of image correlation between the two measurement epochs and visual inspection of the repeat orthoimages point to a highly coherent surface deformation in the inner circles, and reduced image correlation values on the outer ridges are due to stones or groups of stones sliding or tipping individually without coherence over larger areas. However, over the observational period the velocity pattern found is less homogenous than expected from above numerical model and velocity magnitudes seem not to be governed by slope gradient alone. These spatial variations of surface velocities and thus potential un-symmetric mass flux could lead to an un-symmetric development of circle shapes, as indeed also found in nature.

Elevation on the circles is stable or slightly rising by up to 0.7 cm yr^{-1} in the circle centre and on the inner slopes of the surrounding ridges, but lowering up to 1.5 cm yr^{-1} at the outer parts of the inner, fine-domain circle areas and the directly adjacent lower slopes of the course-domain ridges (Fig. 9). In this zone, most material submergence is expected. The short-term change of microrelief found cannot be sustained over longer time scales as slopes would else oversteepen. Thus, the observed changes in topography suggest processes other than a stable convection-like circulation of material to act in addition. Our observation period is too short to allow drawing further conclusions about the nature of such potential processes. Internal variations of the dynamical processes within the circle bodies could play a role as well as (sporadic) external processes of slope adjustment. The development found over Augusts 2007–2010 could be abnormal in relation to average long-term conditions, for instance in response to changes in the active layer thickness and properties. Also, the topographic conditions found in Augusts 2007 and 2010 might deviate from the topographic conditions governing the surface movements, for instance due to differential seasonal frost heave and thaw settlement over the circles. The magnitudes of these seasonal topographic changes could in parts substantially exceed the 3 yr topographic changes (Hallet, 1998).

An observation time period longer than the 3 yr used here might thus be advantageous. On the other hand, it is very likely that the actual dynamics respond to changes in surface and subsurface conditions caused by differences in meteorological conditions from year to year, as well as any long-term trend in climatic conditions. Such non-stationarity might add difficulties with interpretation of the dynamics revealed by long time-lapse data collection. The notable changes in microrelief of the investigated sorted circles as well as the lack of linear correspondence between surface slope and displacement direction and magnitude rather suggest that our study should be followed up, using the same methodology, both by more long term year-to-year monitoring and short-term measurements within a freeze-thaw season. Also, the trends in displacement fields at scales larger than a single circle suggest that such monitoring should include a larger area.

Acknowledgements. We are very grateful to Jaran Wasrud and Tormod Urke for their assistance during field work. The Norwegian Polar Institute provided logistical support. Trond Eiken helped with analysis of the GNSS data. Ground temperature data from Janssonhaugen were kindly made available by Ketil Isaksen, Norwegian Meteorological Institute. This study was funded by the Svalbard Science Forum (RIS 407 DIPGLOW) and the Research Council of Norway (Proj. nos. 446461, RIS 3646 CAPP-dyn and 185906). The software MicMac was kindly provided by the French National Institute of Geographic and Forest Information (IGN).

Author contributions. A. Kääb designed the study, performed the data analysis and wrote the paper. L. Girod constructed the photogrammetric models and products, and edited the paper. I. Berthling designed the study and wrote the paper.

References

Anderson, S. P.: Upfreezing in sorted circles, Western Spitsbergen, 5th International Conference on Permafrost, Trondheim, Norway, 666–671, 1988.

Bockheim, J. G.: Importance of cryoturbation in redistributing organic carbon in permafrost-affected soils, Soil Sci. Soc. Am. J., 71, 1335–1342, doi:10.2136/sssaj2006.0414N, 2007.

Bockheim, J. G., Walker, D. A., Everett, L. R., Nelsen, F. E., and Shiklomanov, N. I.: Soils and cryoturbation in moist nonacidic and acidic tundra in the Kuparuk river basin, Arctic Alaska, USA, Arctic Alpine Res., 30, 166–174, doi:10.2307/1552131, 1998.

Christiansen, H. H., Etzelmuller, B., Isaksen, K., Juliussen, H., Farbrot, H., Humlum, O., Johansson, M., Ingeman-Nielsen, T., Kristensen, L., Hjort, J., Holmlund, P., Sannel, A. B. K., Sigsgaard, C., Åkerman, H. J., Foged, N., Blikra, L. H., Pernosky, M. A., and Ødegård, R.: The thermal state of permafrost in the Nordic area during the International Polar Year 2007–2009, Permafrost Periglac., 21, 156–181, doi:10.1002/ppp.687, 2010.

Etzelmuller, B. and Sollid, J. L.: The Role of weathering and pedological processes for the development of sorted circles on Kvadehuksletta, Svalbard – a short report, Polar Res., 9, 181–191, 1991.

Fonstad, M. A., Dietrich, J. T., Courville, B. C., Jensen, J. L., and Carbonneau, P. E.: Topographic structure from motion: a new development in photogrammetric measurement, Earth Surf. Proc. Land., 38, 421–430, doi:10.1002/Esp.3366, 2013.

Girod, L.: The use of SfM technologies in geosciences: MicMac for geologists, ENSG intership report, 32 pp., 2012.

Hallet, B.: Measurement of soil motion in sorted circles, western Spitsbergen, 7th International Concerence on Permafrost, Yellowknife, 415–420, 1998.

Hallet, B. and Prestrud, S.: Dynamics of periglacial sorted circles in Western Spitsbergen, Quaternary Res., 26, 81–99, 1986.

Hallet, B., Anderson, S. P., Stubbs, C. W., and Gregory, E. C.: Surface soil displacement in sorted circles, Western Spitsbergen, 5th International permafrost conference, Trondheim, Norway, 770–775, 1988.

Heid, T. and Kääb, A.: Evaluation of existing image matching methods for deriving glacier surface displacements globally from optical satellite imagery, Remote Sens. Environ., 118, 339–355, doi:10.1016/j.rse.2011.11.024, 2012.

Horwath, J. L., Sletten, R. S., Hagedorn, B., and Hallet, B.: Spatial and temporal distribution of soil organic carbon in nonsorted striped patterned ground of the High Arctic, J. Geophys. Res.-Biogeo., 113, G03s07, doi:10.1029/2007jg000511, 2008.

Isaksen, K., Benestad, R. E., Harris, C., and Sollid, J. L.: Recent extreme near-surface permafrost temperatures on Svalbard in relation to future climate scenarios, Geophys. Res. Lett., 34, L17502, doi:10.1029/2007gl031002, 2007a.

Isaksen, K., Sollid, J. L., Holmlund, P., and Harris, C.: Recent warming of mountain permafrost in Svalbard and Scandinavia, J. Geophys. Res.-Earth, 112, F02s04, doi:10.1029/2006jf000522, 2007b.

James, M. R. and Robson, S.: Straightforward reconstruction of 3-D surfaces and topography with a camera: accuracy and geoscience application, J. Geophys. Res.-Earth, 117, F03017, doi:10.1029/2011jf002289, 2012.

Kessler, M. A., Murray, A. B., Werner, B. T., and Hallet, B.: A model for sorted circles as self-organized patterns, J. Geophys. Res.-Sol. Ea., 106, 13287–13306, 2001.

Kessler, M. A. and Werner, B. T.: Self-organization of sorted patterned ground, Science, 299, 380–383, 2003.

Kääb, A.: Correlation Image Analysis software (CIAS), available at: http://www.mn.uio.no/icemass, last access: 14 December 2013.

Kääb, A. and Vollmer, M.: Surface geometry, thickness changes and flow fields on creeping mountain permafrost: automatic extraction by digital image analysis, Permafrost Periglac., 11, 315–326, 2000.

Kääb, A., Gudmundsson, G. H., and Hoelzle, M.: Surface deformation of creeping mountain permafrost, photogrammetric investigations on rock glacier Murtèl, Swiss Alps, 7th International Permafrost Conference, Yellowknife, Canada, 531–537, 1998.

Marsz, A. A., Styszynska, A., Pekala, K., and Repelewska-Pekalowa, J.: Influence of meteorological elements on changes in actice-layer thickness in the Bellsund region, Svalbard, Permafrost Periglac., 24, 304–312, doi:10.1002/ppp.1790, 2013.

Matsuoka, N., Abe, M., and Ijiri, M.: Differential frost heave and sorted patterned ground: field measurements and a laboratory experiment, Geomorphology, 52, 73–85, 2003.

MicMac: Documentation, available at: https://geoportail.forge.ign.fr/hg/culture3d/file/c4223bbd9d54/Documentation/, last access: 14 December 2013a.

MicMac: available at: http://logiciels.ign.fr/?-Micmac, last access: 14 December 2013.

Peterson, R. A.: Stability analysis and numerical simulation of differential frost heave, 40, 277–298, doi:10.1007/s11004-008-9150-z, 2008.

Peterson, R. A. and Krantz, W. B.: Differential frost heave model for patterned ground formation: corroboration with observations along a North American arctic transect, J. Geophys. Res.-Biogeo., 113, G03S04, doi:10.1029/2007JG000559, 2008.

Pierrot-Deseilligny, M. and Clery, I.: Recent evolution in photogrammetry and 3d modelisation of natural spaces, Université de Savoie, Collection EDYTEM, 12, 51–66, 2011.

Pierrot-Deseilligny, M. and Clery, I.: Some Possible Protocols of Acquisition for Optimal Use of the “APERO” Open Source Software in Automatic Orientation and Calibration, Castelldefels, Spain, Tutorial, EuroCOW workshop, 8–10 February 2012.

Putkonen, J.: Soil thermal properties and heat transfer processes near Ny-Alesund, northwestern Spitsbergen, Svalbard, Polar Res., 17, 165–179, 1998.

Schmertmann, J. and Taylor, R. S.: Quantitative Data from a Patterned Ground Site over Permafrost, US Army Cold Regions and Engineering Laboratory, Hanover, NH, 1965.

Tolgensbakk, J. and Sollid, J. L.: Kvadehuksletta, Geomorfologi og kværtærgeologi 1 : 10000, Norsk Polarinsitutt, Oslo, 1987.

Washburn, A. L.: Geocryology. A survey of Periglacial Processes and Environments, John Wiley, Washington/New York, 406 pp., 1980.

Westoby, M. J., Brasington, J., Glasser, N. F., Hambrey, M. J., and Reynolds, J. M.: “Structure-from-Motion” photogrammetry: a low-cost, effective tool for geoscience applications, Geomorphology, 179, 300–314, doi:10.1016/j.geomorph.2012.08.021, 2012.

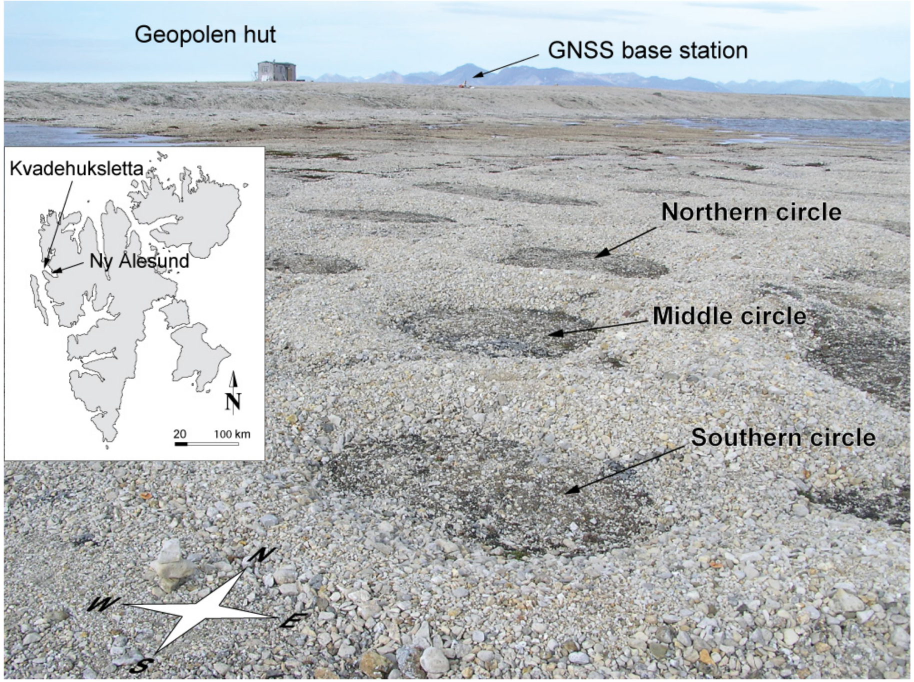

Fig. 1. Photo of site and sorted circles studied with inset map of Svalbard. The darker, inner parts of the circles have a diameter of around 1.5 m on average. View to the north.

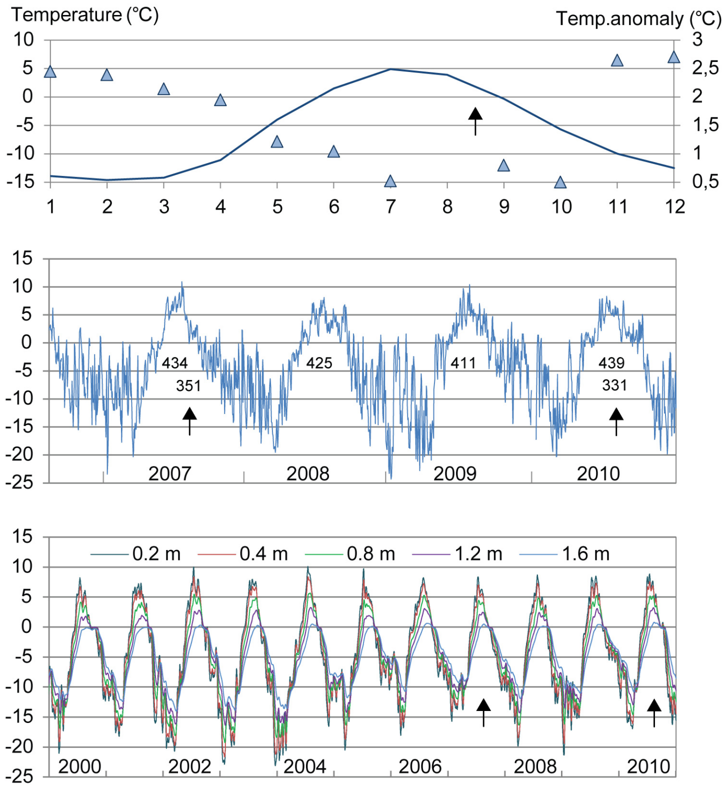

Fig. 2. (Upper) mean monthly air temperature in Ny-Ålesund for the 1961–1990 normal period (solid line). Temperature anomaly for all months calculated as a mean of monthly deviations from normal during the 1991–2010 period (triangles). (Middle) air temperature in Ny-Ålesund during the September 2006 – December 2010 period. Degree day sum during summers 2007–2010 displayed within the graph; sum at the time of photography in 2007 and 2010 below. (Lower) ground temperatures from the shallow Janssonhaugen borehole. Photography dates indicated as arrows.

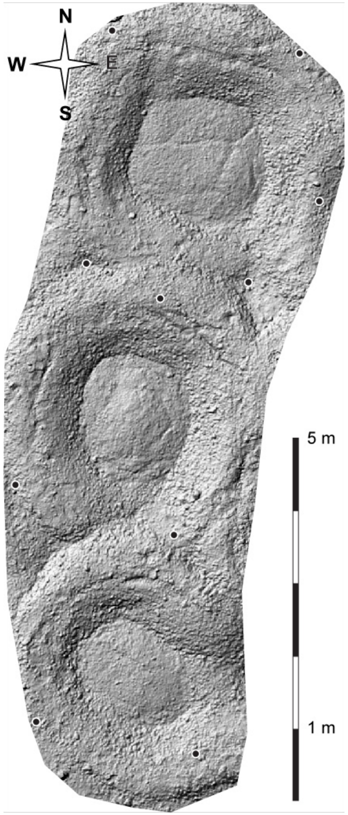

Fig. 3. Shaded relief (hillshade) of the 2007 DEM, resampled to 2 cm resolution, over the three sorted circles. Black dots indicate the positions of the ground control points used. Note the soil cracks on the ridge tops and in the inner domains.

Fig. 4. Section of the 2010 orthophoto (left) and DEM hillshade (right). Southwestern part of the northern sorted circle. White contour lines indicate 2 cm elevation differences.

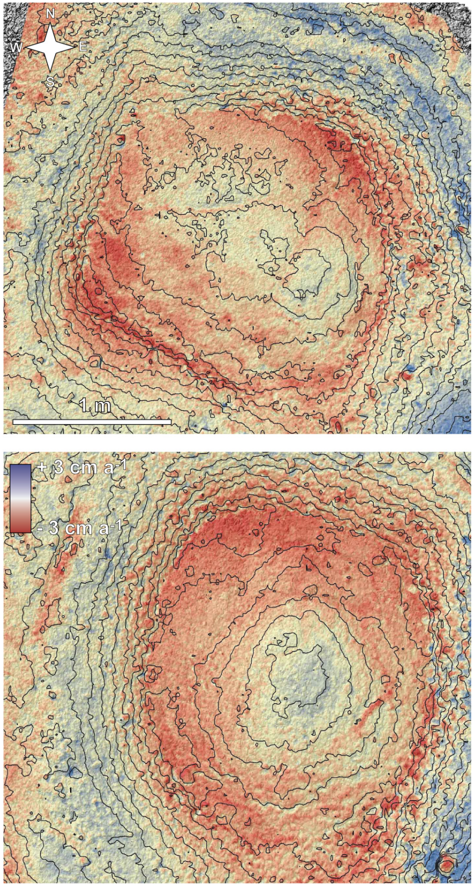

Fig. 5. Elevation change 2007–2010 on the northern (top) and middle circle (bottom). 2 cm contour lines are indicated in black. The highest parts of the inner domains coincide well with the largest rates of surface heave in this domain, and the deepest parts with the strongest surface lowering.

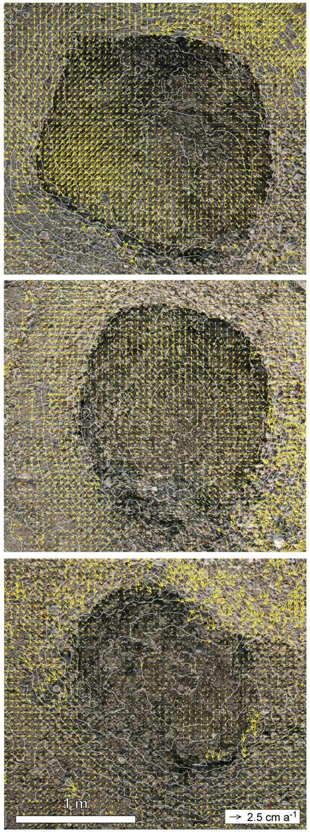

Fig. 6. Horizontal surface displacements 2007–2010 on all three circles. Chaotic vectors or groups of vectors are typically caused by individual stones that slide or tip, but could in some cases also be mismatches. Measurements with very low correlation coefficients have been removed. Linear vector scale with maximum vector magnitude of 2.5 cm yr^{-1}.

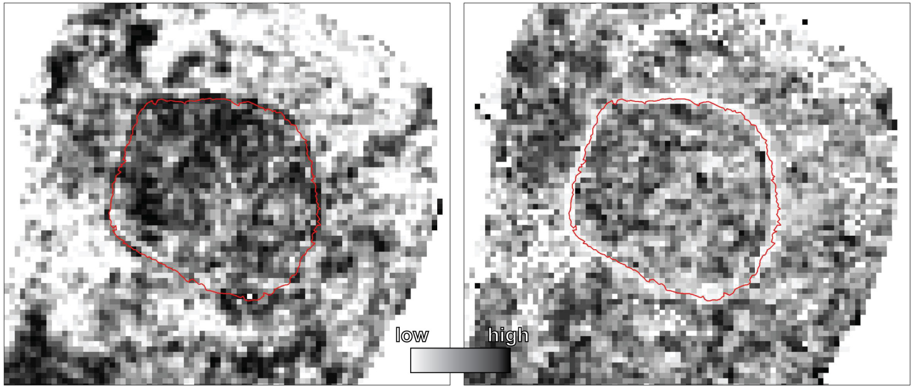

Fig. 7. Northern circle. Maximum correlation coefficients (left) and signal-to-noise ratio (SNR; right) of the image matching of Fig. 6. SNR is defined as the ratio between the maximum correlation coefficient and the average correlation coefficient for each individual match. Transition between inner domain and surrounding ridge indicated in red.

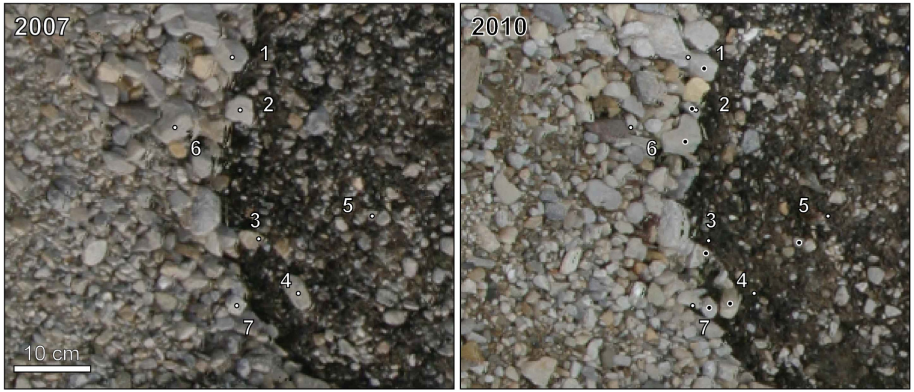

Fig. 8. Section of 2007 and 2010 orthoimages to the southwest of the northern circle. 2007 positions of selected stones are marked by white dots (left and right), 2010 positions of the corresponding stones by black dots (right). Stones 1–3 are in the process of being incorporated into the base of the course-grained ridges. Stones 4 and 5 move outwards from the circle centre. Stones 6 and 7 fell/slided down the ridge.

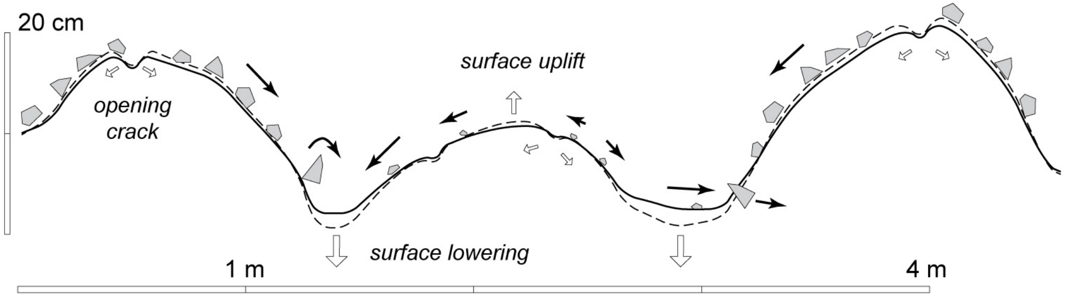

Fig. 9. Sketch summarizing the findings of the study. The topographic profile shown is approximately a southwest to northeast cross-section over the centre of the middle circle with height exaggerated. The solid line indicates time 2007, the dashed line 2010. Black arrows indicate soil surface movement, the white arrows surface elevation changes.